Nonlinear Processes in Geophysics (1997) 4: 173–183

Nonlinear Processes in Geophysics


# Width dependent collisionless electron dynamics in the static fields of the shock ramp, 2, Phase space portrait

**M. Gedalin[1], U. Griv[1], and M.A. Balikhin[2]**

[1]Ben-Gurion University, Beer-Sheva, Israel
[2]Sheffield University, Sheffield, England

Received: 22 October 1997 – Accepted: 26 February 1998

**Abstract.** We study numerically in detail the behavior of electrons in the strongly inhomogeneous static magnetic and electric fields, which are typical for thin quasiperpendicular collisionless shocks. We pay particular attention to the dependence of the final electron velocities on their initial velocities, for different shock widths. Electrons are completely magnetized when the shock is wide, but become demagnetized, and the energies that they acquire rapidly increase with the steepening of the field structure. One of the clear manifestations of the electron demagnetization is the loss of even approximate one-to-one correspondence of the downstream perpendicular velocity to the upstream perpendicular velocity. Electron reflection occurs despite the large cross-shock potential which accelerates electrons along the magnetic field (the regime of complete magnetization) or across the shock (strong demagnetization). The reflected ion fraction is sensitive to the potential, magnetic field jump, and ramp width.

## 1 Introduction

In the present paper we continue the studies of the charged particle behavior is strongly inhomogeneous electric and magnetic fields, typical for oblique shock profiles. It has been known (Balikhin et al., 1993; Cole, 1976; Gedalin et al. , 1995b; Rothwell et al, 1995) that the charged particle motion in sufficiently inhomogeneous $\mathbf{E} \perp \mathbf{B}$ may become demagnetized even if the typical inhomogeneity scale it larger then the particle thermal $v_\perp/\Omega$ (where $\Omega = eB/mc$) and convective $v_d/\Omega$ (where $v_d$ is the particle drift velocity across the magnetic field) gyroradii. This fact was used by Balikhin et al. (1997, 1993); Balikhin and Gedalin (1994); Gedalin et al. (1995c) to the explanation of strong prompt perpendicular electron heating at quasiperpendicular collisionless shocks. The mechanism is efficient for strong electric field gradients and subsonic incident electron distribution in the de Hoffman-Teller frame (Gedalin et al., 1995a,c). Its natural continuation onto the wide shock or hot initial electron distribution regimes is the well-known mechanism of electron heating due to their acceleration along the magnetic field by the de Hoffman-Teller cross-shock potential (Feldman et al., 1982; Feldman, 1985; Schwartz et al., 1988; Scudder, 1995; Scudder et al., 1986c; Thomsen et al., 1987a). The electron demagnetization is sensitive to the fine structure of the shock front, which is not studied very well so far, and especially to the details of the electric field behavior. The last is rarely available with sufficient resolution and if available (Formisano, 1982; Wygant et al., 1987). In both limits (thin shock with demagnetization and thick shock with acceleration along the magnetic field) it is usually assumed that the shock structure is one-dimensional and stationary. The very definition and transition between the normal incidence frame (where the incident plasma flow is along the shock normal) and the de Hoffman-Teller frame (where the incident plasma flow is along the upstream magnetic field) makes physical sense if the structure is one-dimensional and stationary, at least within some appropriate approximation.

Gedalin et al. (1995b) have shown that in the one dimensional stationary structure the drastic transition from complete magnetization to strong demagnetization occurs when $\lambda = e|dE_x/dx|/m_e\Omega_e^2 \gtrsim 1$. Using the equation of motion with the massless electron approximation, one has in the normal incident frame

$$eE_x = -\frac{1}{n}\frac{dp_{e,xx}}{dx} - \frac{e}{c}\hat{\mathbf{n}}\cdot(\mathbf{V}_e \times \mathbf{B}), \qquad (1)$$

where the first part in the right hand side represents the de Hoffman-Teller electric field, $p_{e,xx}$ and $n$ are the electron pressure and number density, respectively, $\hat{\mathbf{n}}$ is the unit vector along the shock normal, and $\mathbf{V}_e$ is the electron current velocity. If the electron current dominates and the electron pressure anisotropy is weak, this expression take the following approximate form:

$$eE_x \approx -\frac{1}{n}\frac{d}{dx}\left(p_e + \frac{B^2}{8\pi}\right). \qquad (2)$$

*Correspondence to:* Department of Physics, Ben-Gurion University, P.O. Box 653, Beer-Sheva, 84105, Israel

Scudder et al. (1986a,b,c) argued that the ion current may be non-negligible, but the de Hoffman-Teller cross-shock potential is substantially smaller than the normal incidence frame potential. As a first order approximation we shall estimate the demagnetization parameter using (2). Thomsen et al. (1987a) found that in the shock with weak electron heating $p_e \propto n^\gamma$, $\gamma \approx 2$, while in the case of the strong heating $\gamma > 2$. Scudder et al. (1986b) argued that $n/B \approx$ const across the shock. Using these approximations we find the cross-shock potential

$$s = \frac{2e\varphi}{m_i V_u^2} \approx \frac{(1+\beta_e)(B_d/B_u - 1)}{M^2}, \qquad (3)$$

where $B_u$ and $B_d$ are the magnetic fields at the upstream and downstream edges of the ramp. If the ramp width is $L$, and we assume for the electric field a triangle profile with the maximum approximately in the middle of the ramp, one finds

$$\lambda \approx \frac{2(1+\beta_e)(B_d/B_u - 1)}{(\omega_{pe}L/c)^2}. \qquad (4)$$

For the low Mach number 77 Nov 26, 0610 UT shock the approximation (2) should be quite appropriate (Gedalin, 1996; Newbury et al., 1997a), although the found $L \approx (c/\omega_{pi})$ underestimates the magnetic field gradient in the ramp by a factor of $\approx 1.2$. Using the parameters of the shock ($M = 2.7$, $\beta_e = 0.36$, and $B_d/B_u \approx 3$, one finds $\lambda \approx 0.003 \ll 1$, which perfectly agrees with our understanding that electrons are completely magnetized in low Mach number shocks. For the high Mach number 77 Nov 7, 2251 shock the ramp width is estimated to be $2 < L/(c/\omega_{pe}) < 8$ (Scudder et al., 1986a). Using for our estimate $L \approx 6(c/\omega_{pe})$ and the shock parameters $B_d/B_u \approx 5$, $\beta_e = 1.6$, one finds $\lambda \approx 0.6$, which is marginal, taking into account the uncertainties of our knowledge of the actual electric field distribution inside the ramp. For the thin, high Mach number, 80 Aug 1, 2135 shock the ramp width is as small as only $2(c/\omega_{pe})$ (Newbury and Russell, 1996), and using $B_d/B_u \approx 3$, $\beta_e \approx 0.5$, one finds $\lambda \approx 2.25$, which is well into the demagnetization regime.

Given the lack of the knowledge of the electric field profile in the shock front, it is impossible to make any general conclusion as to whether the demagnetization is a common or an exceptional effect. Recent full-particle numerical simulations (Krauss-Varban et al., 1995; Liewer et al., 1991; Savoini and Lembege, 1994) are not unambiguous. Explicit code simulations with higher mass-ratio (Liewer et al., 1991; Savoini and Lembege, 1994) ($m_i/m_e = 400$ and in several cases $m_i/m_e = 1600$) show strong electron heating associated with the high gradients of electric field, but these simulations cannot be run for sufficiently long time to produce a stable shock profile. Implicit code simulations with lower mass ratio show weak heating close to what is expected in the adiabatic regime (complete magnetization), but have been unable so far to reproduce observed strong heating regimes.

The situation is even more complicated due to the evidence of a three-dimensional structure of the shock front in the ramp vicinity (Scudder et al., 1986a), which is confirmed by presence of large amplitude fluctuations of the normal component of the magnetic field (which is supposed to be constant in the one-dimensional stationary case). Oscillating shock front or small-scale large amplitude moving structures inside the shock (Gedalin et al., 1998; Newbury et al., 1997b) also do not conform the usual assumptions of one-dimensionality of stationarity of the shock front, nor does the reforming front of a very high Mach number shock (Quest, 1985). Yet all this cases have in common a strongly inhomogeneous $\mathbf{E} \perp \mathbf{B}$. Since the fields are slowly varying at the typical electron timescale $1/\Omega_e$, one can expect that electron motion in these structures will be qualitatively similar to what happens in a thin shock front. Therefore, modeling electron dynamics in the shock front, one can shed light on the electron interaction with large-amplitude thin nonstationary structures.

In the absence of a satisfactory description of the fine structure of the shock front, we shall analyze the electron motion in a model field structure. In the accompanying paper (Gedalin and Balikhin, 1998) we study the electron trajectories and downstream parallel and perpendicular electron heating as a function of the shock width. In the present paper we study in detail the effects of the demagnetization of the electron distribution within the shock profile, paying particular attention to the determination of which electrons undergo this transition and how their final velocities depend on the initial ones. The paper is organized as follows. In section 2 we revisit the cross-shock potential taking into account possible shock non-stationarity and deviations from the one-dimensional structure. In section 3 we consider briefly the local behavior of electron trajectories in a general inhomogeneous fields and derive approximate criterion for the electron demagnetization. The purpose of this analysis is to generalize the conclusions onto other possible configurations with sharp gradients of electric field perpendicular to the magnetic field, irrespectively of their stationarity and one-dimensionality. We show that demagnetization is a general feature if these configurations, which means that it may occur in time-dependent and/or three-dimensional shock profile as well. In section 4 we perform numerical analysis of electron trajectories in a model shock profile and consider the Liouville mapping of initial velocities into final ones, $\mathbf{v}_i \rightarrow \mathbf{v}_f$, for different ramp width. We use an oversimplified shock model for the following reasons. First, lack of detailed knowledge about the shock structure makes insensible any attempt to refine the model. Second, as is shown by Gedalin et al. (1995b), substantial electron demagnetization occurs only within the most narrow parts of the shock front (ramp). In other parts electrons behave adiabatically. Although the electron motion in these parts would affect the final distribution it is unimportant for the study of demagnetization properties, which is of interest here.

## 2 Cross-shock potential revisited

The collisionless shock profile is usually assumed one-dimensional and stationary, for theoretical purposes and interpretation of observations, even when it is quite clear that it is not so (Scudder et al., 1986a). This approximation has been widely used for the description and comparison of the electron motion in different frames (Goodrich and Scudder, 1984). If we assume that the shock normal may be defined properly (that is, there exists a direction, along which spatial variations are in average much stronger, than in the transverse direction), the normal incidence frame (N) and de Hoffman-Teller frame (HT) are well defined (de Hoffman and Teller, 1950). To be specific we shall choose this shock normal along $x$ axis, and $xz$ plane as the coplanarity plane. Then the relative velocity of the two frames is $\mathbf{V}_r = V_u(0,0,\tan\theta)$, where $V_u$ is the upstream plasma velocity in the normal incidence frame (directed in the positive $x$ direction), and $\theta$ is the angle between the shock normal and upstream magnetic field. The relation between the N and HT electric fields is

$$\mathbf{E}^{(N)} = \mathbf{E}^{(HT)} + \frac{1}{c}\mathbf{V}_r \times \mathbf{B}, \tag{5}$$

where we assume that all velocities and nonrelativistic. In the one-dimensional stationary case $B_x = B_u\cos\theta = \text{const}$, $E_y^{(N)} = V_u B_x/c = \text{const}$, and $E_y^{(HT)} = 0$. When the profile is not one-dimensional or nonstationary, neither $B_x$ nor $E_y$ are necessarily constant, and $E_y^{(HT)} \neq 0$, in general.

The general expression for the electric field is usually obtained from the hydrodynamical equation of motion for electrons (Scudder et al., 1986b):

$$e\mathbf{E} = -\frac{1}{n_e}\nabla\cdot\overleftrightarrow{P}_e - \frac{e}{c}\mathbf{V}_e\times\mathbf{B} - m_e\frac{d\mathbf{V}_e}{dt}, \tag{6}$$

where $\mathbf{V}_e$ is the electron fluid velocity, $\overleftrightarrow{P}_e$ is the electron pressure tensor, and $d/dt = (\partial/\partial t) + \mathbf{V}_e\cdot\nabla$ is the total derivative. It is usually assumed that the electron pressure is isotropic and their mass can be neglected. In this approximation (6) takes a simpler form:

$$e\mathbf{E} = -\frac{1}{n_e}\nabla P_e - \frac{e}{c}\mathbf{V}_e\times\mathbf{B}. \tag{7}$$

It should be emphasized that (6)-(7) are written in the arbitrary frame and are equally valid in N and HT as well. Projecting (7) onto the magnetic field direction, one finds the electric field component, parallel to the local magnetic field, as follows:

$$eE_\parallel = -\frac{1}{n_e}\mathbf{b}\cdot\nabla P_e, \tag{8}$$

where $\mathbf{b} = \mathbf{B}/|\mathbf{B}|$. This expression is especially useful if the shock is one-dimensional and stationary, giving immediately

$$eE_x^{(HT)} = \frac{eE_\parallel^{(HT)}}{\cos\theta} = -\frac{1}{n_e}\frac{dP_e}{dx}, \tag{9}$$

$$e\varphi^{(HT)} = \int\frac{1}{n_e}\frac{dP_e}{dx}dx, \tag{10}$$

$$e\varphi^{(N)} = \int\left(\frac{1}{n_e}\frac{dP_e}{dx} + \frac{V_u B_y\tan\theta}{c}\right)dx - \frac{eV_u B_u\sin\theta}{c}y. \tag{11}$$

The relations (9)-(11) have been extensively used for the description of electron motion within the shock front. Eq. (10), in particular, provides the useful energy conservation relation since the potential depends only on $x$. It is worth mentioning, however, that relations are only approximations, and if substantial wave activity is superimposed on a stationary ramp or the ramp itself it a three-dimensional structure, none of the above assumptions (one-dimensionality and stationarity) is correct, and $\mathbf{E}^{(HT)}\cdot\mathbf{B} \neq E_x^{(HT)}B_x$, so that (9) no longer applies. Inside the narrow ramp transition, where the spatial scale of the variation in $x$ direction may be assumed significantly smaller than in $y$ and $z$ directions, (7) can be simplified a little. From the current equation (neglecting the displacement current for typical velocities much smaller than the light speed and assuming quasineutrality) one has

$$\mathbf{V}_e = \mathbf{V}_i - \frac{c}{4\pi ne}\nabla\times\mathbf{B}. \tag{12}$$

The effective current velocity in $y$ direction is

$$V_{y,\text{eff}} \sim \frac{c}{4\pi ne}\frac{B_d - B_u}{L}, \tag{13}$$

where we ignored the insignificant here difference between $B_z$ and $|\mathbf{B}|$ for quasiperpendicular shocks and $L$ is the ramp scale. The maximum $y$ component of the velocity of a reflected ion is $\sim V_u$ (in the normal incident frame), and the hydrodynamic ion velocity cannot exceed $\sim \alpha V_u$, where $\alpha$ is the reflected ion fraction(usually 20-30% for high Mach number supercritical shocks), so that

$$\frac{V_{y,\text{eff}}}{V_{i,y}} \sim \frac{c(B_d/B_u - 1)}{\alpha M\omega_{pi}L} \tag{14}$$

and is large for typical ramp scales $L \sim 0.2(c/\omega_{pi})$ and $B_d/B_u \sim M$. Therefore, we can neglect $V_{i,y}$ in (12) and substituting $\mathbf{V}_e \approx -(c/4\pi ne)\nabla\times\mathbf{B}$ further into (7) one has

$$eE_x^{(N)} \approx -\frac{1}{n}\frac{d}{dx}\left(P_e + \frac{B^2}{8\pi}\right). \tag{15}$$

We emphasize that $B$ is the total magnetic field, including the superimposed nonstationary wave fields, and (15) is the appropriate approximation, even if the overall structure if not one-dimensional and nonstationary. It is based only on the local pressure balance for light electrons, taking into account

that the ion current is limited, $|j_i| \lesssim nV_u$, and is by far insufficient to produce large magnetic field gradients. It is worthwhile to mention also that the above approximation should work also when the deviations from one-dimensionality are substantial, in which case the derivative with respect to $x$ should be substituted by the derivative along the highest gradient direction.

## 3 Electron trajectories: local analysis

Local trajectory analysis was comprehensively done for the case of a stationary one-dimensional shock profile (Gedalin et al., 1995a; Gedalin and Balikhin, 1998). Here we generalize the analysis onto the case of slowly time varying but otherwise arbitrary fields. The electron motion in the shock ramp is governed by the following equations of motion:

$$m_e\frac{d\mathbf{v}}{dt} = -e\mathbf{E} - \frac{e}{c}\mathbf{v}\times\mathbf{B}, \quad \frac{d\mathbf{r}}{dt} = \mathbf{v}, \tag{16}$$

where the electric and magnetic fields are functions of coordinates $\mathbf{r}$ and time $t$. In the spirit of Balikhin et al. (1993), let us consider the evolution of the two initially close trajectories $\mathbf{r}(t)$ and $\mathbf{r}'(t)$. Assuming that $\delta\mathbf{r}(t) = \mathbf{r}'(t) - \mathbf{r}(t)$ is small, we Taylor expand the equations of motion to obtain

$$m_e\frac{d\delta\mathbf{v}}{dt} = -e(\delta\mathbf{r}\cdot\boldsymbol{\nabla})\mathbf{E} - \frac{e}{c}\delta\mathbf{v}\times\mathbf{B} - \frac{e}{c}\mathbf{v}\times(\delta\mathbf{r}\cdot\boldsymbol{\nabla})\mathbf{B}, \tag{17}$$

$$\frac{d\delta\mathbf{r}}{dt} = \delta\mathbf{v}. \tag{18}$$

Being interested in fast changes of $\delta\mathbf{r} \propto \exp(\lambda t)$, where $\lambda \gtrsim \Omega_e = eB/m_ec$, we shall neglect the dependence of the fields on time in (17)-(18). This approximation should be appropriate even for wave fields if their frequencies are much lower than the electron gyrofrequency $\Omega_e$. For the present local analysis $\mathbf{v}(t)$ should be treated as a constant parameter. Then (17) can be written as follows:

$$\frac{d\delta\mathbf{v}}{dt} = -\frac{e}{m_e}(\delta\mathbf{r}\cdot\boldsymbol{\nabla})\mathbf{E}' - \delta\mathbf{v}\times\boldsymbol{\Omega}_e, \tag{19}$$

where $\mathbf{E}' = \mathbf{E} + \mathbf{v}\times\mathbf{B}/c$ is the electric field in the instantaneous comoving frame, and $\boldsymbol{\Omega}_e = e\mathbf{B}/m_ec$ is the instantaneous gyrofrequency vector. Now, substituting $d/dt \to \lambda$, one arrives at the following linear homogeneous equation

$$\lambda^2\delta\mathbf{r} + (e/m_e)(\delta\mathbf{r}\cdot\boldsymbol{\nabla})\mathbf{E}' - \lambda\delta\mathbf{r}\times\boldsymbol{\Omega}_e = 0, \tag{20}$$

and $\lambda$ is determined from the following equation:

$$\det\|\lambda^2\delta_{ij} + (e/m_e)\nabla_jE'_i + \lambda\epsilon_{ijk}\Omega_{e,k}\| = 0, \tag{21}$$

where $\delta_{ij}$ is the Kronecker tensor, $\epsilon_{ijk}$ is the Levy-Chivita tensor, $\nabla_i = \partial/\partial x_i$, and summation is implied on $k$. This equation is a sixth order equation for $\lambda$ of the following kind:

$$\lambda^6 + A_4\lambda^4 + A_3\lambda^3 + A_2\lambda^2 + A_1\lambda + A_0 = 0, \tag{22}$$

where

$$A_4 = \frac{e}{m_e}\boldsymbol{\nabla}\cdot\mathbf{E}' + \boldsymbol{\Omega}_e^2, \tag{23}$$

$$A_3 = -\frac{e}{m_ec}\boldsymbol{\Omega}_e\cdot\dot{\boldsymbol{\Omega}}_e, \tag{24}$$

$$A_2 = \frac{e^2}{2m_e^2}[(\boldsymbol{\nabla}\cdot\mathbf{E}')^2 - (\nabla_iE'_j)(\nabla_jE'_i)] + \frac{e}{m_e}\boldsymbol{\Omega}_e\cdot(\boldsymbol{\Omega}_e\cdot\boldsymbol{\nabla})\mathbf{E}', \tag{25}$$

$$A_1 = -\frac{e}{m_ec}\boldsymbol{\Omega}_e(\dot{\boldsymbol{\Omega}}_e\cdot\boldsymbol{\nabla})\mathbf{E}', \tag{26}$$

$$A_0 = \frac{e^3}{m_e^3}\epsilon_{ijk}(\nabla_xE'_i)(\nabla_yE'_j)(\nabla_zE'_k), \tag{27}$$

where dot means the time derivative in the electron instantaneous comoving frame $\dot{(\dots)} = (\partial/\partial + \mathbf{v}\cdot\boldsymbol{\nabla})(\dots)$, and we have used the Maxwell equation $\boldsymbol{\nabla}\times\mathbf{E} = -(1/c)\partial\mathbf{B}/\partial t$. It is easy to see that there is always at least one root with $\mathrm{Re}\,\lambda > 0$, unless $A_3 = A_1 = 0$ and $A_4 \geq 0$, $A_2 \geq 0$, and $A_0 \geq 0$ (cf. Balikhin et al., 1997) (these conditions are necessary for absence of $\mathrm{Re}\,\lambda > 0$ but not sufficient). Therefore, trajectory divergence is quite typical for inhomogeneous systems.

As was pointed out by Balikhin et al. (1997) (see also Gedalin and Balikhin (1998)), local trajectory divergence does not necessarily means demagnetization. We shall consider several special cases first.

*Parallel inhomogeneity regime.* In this case $\mathbf{B} = (0, 0, B_z) = \mathrm{const}$ and $\mathbf{E} = (E_x, E_y, E_z(z))$, where $E_x$ and $E_y$ are constant. It is easy to see that (22) takes the form:

$$\lambda^6 + (\frac{e}{m_e}\frac{\partial E_x}{\partial x} + \Omega_e^2)\lambda^4 + \Omega_e^2\frac{e}{m_e}\frac{\partial E_x}{\partial x}\lambda^2 = 0, \tag{28}$$

and the trajectories diverge if $\partial E_x/\partial x < 0$. However, the equations of motion (16) take the following simple form:

$$m_e\frac{dv_x}{dt} = -eE_x - \frac{e}{c}v_yB_z, \tag{29}$$

$$m_e\frac{dv_y}{dt} = -eE_y + \frac{e}{c}v_xB_z, \tag{30}$$

$$m_e\frac{dv_z}{dt} = -eE_z, \tag{31}$$

so that it is obvious that the motion in the $xy$ plane is the $\mathbf{E}\times\mathbf{B}$ drift with the velocity $\mathbf{V}_d = c(E_y/B_z, -E_x/B_z)$ and gyration with the gyrofrequency $\Omega = eB_z/m_ec$, while along the magnetic field one has energy conservation $\varepsilon = m_ev_z^2/2 - e\phi = \mathrm{const}$, where $E_z = -d\phi/dz$. The corresponding time-independent solution of Vlasov equations would be $f(v_x, v_y, v_z) = F(v_\perp, \varepsilon)$, where $v_\perp^2 = (v_x - V_{dx})^2 + v_y - V_{dy})^2$ is the gyration velocity. In particular, for $f = \mathrm{const}f_1(v_\perp)\exp[-(v_{z0} - V_0)^2/2v_T^2]$ at $\phi = 0$ one finds

$$f = \mathrm{const}f_1(v_\perp) \cdot \exp[-(\sqrt{v_{z0}^2 + 2e\phi/m_e} - V_0)^2/2v_T^2], \tag{32}$$

and it can be easily shown that the parallel temperature is lower (that is, the distribution is *cooled*) in the regions with the higher potential (cf. Gedalin at al., 1996), independently of the $dE_x/dx$.

*Perpendicular geometry, no motional field.* In this case we shall assume $\mathbf{B} = (0, 0, B_z(x))$ and $\mathbf{E} = (E_x(x), 0, 0)$. Absence of the motional field $E_y$ means that there is no electron $\mathbf{E} \times \mathbf{B}$ drift in $x$-direction in the lowest order approximation. Eq.(22) takes the following form:

$$\lambda^6 + (\frac{e}{m_e}\frac{\partial E_x}{\partial x} + \Omega_e^2)\lambda^4 = 0, \tag{33}$$

and the trajectories diverge when $(e/m_e)(\partial E_x/\partial x) + \Omega^2 < 0$, in agreement with Balikhin et al. (1993). In this case the equations of motion are

$$m_e\frac{dv_x}{dt} = -eE_x - \frac{e}{c}v_y B_z, \tag{34}$$

$$m_e\frac{dv_y}{dt} = -\frac{e}{c}v_x B_z, \tag{35}$$

$$m_e\frac{dv_z}{dt} = 0. \tag{36}$$

Eq.(35) is immediately integrated to $m_e v_y + e\mathcal{A}_y = P_y =$ const (conservation of the generalized momentum, corresponding to the ignorable coordinate), where $\mathcal{A}_y = \int B_z dx$. Substituting this to (34) one finds $\varepsilon = m_e v_x^2/2 + U(x) =$ const, where $U = -e\phi + eP_y\mathcal{A}_y/m_e c - e^2\mathcal{A}_y^2/2m_e c^2$ (conservation of time-independent Hamiltonian). The last relation means that the electron velocities (and therefore the distribution function) depend only on the integrated characteristics $\phi$ and $\mathcal{A}_y$ and are independent of the gradients of $\mathbf{B}$ and $E$. It is easily seen that there is no temperature change in $y$ direction, while in $x$ direction temperature changes as in the previous case.

*Oblique geometry model.* In this model (Gedalin et al. , 1995b) the magnetic field is constant $\mathbf{B} = (B_x, 0, B_z) =$ const and the electric field is chosen as $\mathbf{E} = (kx, E_y, 0)$, where $E_y =$ const and $k =$ const. Equations of motion are fully integrable. It was shown (Gedalin et al. , 1995b) that if $k < 0$ the electron trajectory instability occurs and electrons are accelerated across the magnetic field in $x$ direction. Closer analysis of the solutions obtained by (Gedalin et al. , 1995b) shows that when $\lambda t \to \infty$ the electron distribution tends to a monoenergetic beam. In this case the result does depend on $k = dE_x/dx$, but the trajectory divergence itself does not mean heating.

These cases have in common full integrability, namely, the system possesses complete set of integral of motions. More precisely, in all these cases there are sufficient integrals of motion to globally isolate a one-dimensional space in which the unstable vector lies. We, therefore, argue, that the trajectory divergence itself does not result in any heating. The effect is completely nonlinear and apparently requires that the system be non-integrable. In all cases where nonadiabatic heating was found numerically (Balikhin et al., 1993; Gedalin et al., 1995a; Gedalin et al. , 1995b; Gedalin and Balikhin, 1998), is was due to restoration of adiabaticity and efficient conversion of the energy of accelerated demagnetized electron into the gyration energy. Thus, we proceed bearing in mind that the trajectory instability should occur in a part of the structure, being followed by the conversion region with effective magnetization, that is $\mathrm{Re}\,\lambda$ must change its sign from positive to negative in order that the trajectory instability results in heating. This is somewhat similar to the stretching and folding scenario in Hamiltonian chaotic systems (Tabor, 1989), although in our case the motion is not chaotic, and heating is produced in a single demagnetization - magnetization sequence.

As is shown in Balikhin et al. (1997) the trajectory instability occurs even when there is no electric field, solely due to the magnetic field variation. This divergence is related to the adiabatic energization of electrons rather than to the demagnetization, although it "helps" demagnetization by smearing out the boundary between the adiabatic and nonadiabatic regimes and allowing weak demagnetization for smaller electric field gradients. As it is known (Balikhin et al., 1993; Gedalin et al., 1995a), presence of the inhomogeneous electric field, parallel to the magnetic field, substantially weakens the conditions for the demagnetization. In order to analyze the effects of the weak nonstationarity of the fields and of deviations from one-dimensionality, we exclude the two mentioned effects assuming $\mathbf{B} = (0, 0, B_z) =$ const, $E_z = 0$, and $\nabla_z = 0$. It is easy to see, that (22) takes the following simple form:

$$\lambda^2\left[\lambda^4 + \frac{e}{m_e}(\nabla\cdot\mathbf{E} + \Omega_e^2)\lambda^2 - \frac{e}{2m_e c}\frac{d}{dt}\Omega_e^2\lambda + \frac{e^2}{m_e^2}(\frac{\partial E_x}{\partial x}\frac{\partial E_y}{\partial y} - \frac{\partial E_x}{\partial y}\frac{\partial E_y}{\partial x})\right] = 0. \tag{37}$$

When the geometry is planar, that is, $\nabla = \hat{\mathbf{l}}\nabla$, and $\dot{\Omega}_e = 0$ (37) reduces to the condition found by Balikhin et al. (1993). In the general case (37) does not have any roots with $\mathrm{Re}\,\lambda > 0$, if $\dot{\Omega}_e = 0$, $\kappa_1 = \nabla\cdot\mathbf{E} + \Omega_e^2 \geq 0$, $\kappa_2 = (\partial E_x/\partial x)(\partial E_y/\partial y) - (\partial E_x/\partial y)(\partial E_y/\partial x) \geq 0$, and $\kappa_1^2 - 4\kappa_2 \geq 0$. Thus, the condition for the trajectory instability becomes substantially weaker than even in the oblique case where there is inhomogeneous parallel electric field present. To make this conclusion more quantitative, we compare the two cases, for which $\dot{\Omega}_e = 0$ and the electric field is a potential field $\mathbf{E} = -\nabla\phi$: (a) one-dimensional geometry $\phi = \frac{1}{2}kx^2$, and two-dimensional geometry $\phi = \frac{1}{2}k(x^2+y^2)$. It is easy to see that in the one-dimensional case the instability conditions reads $ek/m_e > \Omega_e^2$, while in the two-dimensional case it becomes $ek/m_e > \Omega_e^2/4$, which weakens the requirements to the smallness of the scale of electric field variation.

One can see that in all cases trajectory instability is guaranteed if $(e/m_e)\nabla\cdot\mathbf{E}' + \Omega_e^2 < 0$,. Thus, for semi-quantitative analysis we adopt the following condition for local demag-

netization of electron motion

$$\alpha \equiv -(e/m_e)\nabla \cdot \mathbf{E}'/\Omega_e^2 > 1, \quad (38)$$

which is a three-dimensional generalization of the condition found earlier by Balikhin et al. (1993); Gedalin et al. (1995b) for the case of planar geometry. It is easy to see that this condition places the following restriction on the deviations from quasineutrality in the instantaneous comoving frame:

$$\frac{\delta n}{n} > \frac{\Omega_e^2}{\omega_{pe}^2}. \quad (39)$$

For $n \sim 5\,\mathrm{cm}^{-3}$ and $B = 10\,\mathrm{nT}$, one has $\delta n/n > 4 \cdot 10^{-4}$ for $\lambda > |\Omega_e|$, which is not unreasonable.

To summarize this analysis, electrons become locally demagnetized with very modest deviations from quasineutrality. Such demagnetization is even easily achieved if the geometry is not one-dimensional geometry or stationarity of the electric and magnetic fields. Balikhin et al. (1993); Gedalin et al. (1995b) have shown that such demagnetization results in the electron acceleration across the magnetic field and efficient energy input into the transverse degree of freedom.

## 4 Phase space: numerical analysis

In the previous section we studied local stability of electron trajectories in general (not necessarily one-dimensional and stationary) set of electric and magnetic fields. Although it is relatively easy for an electron to become locally demagnetized, the resulting energization would depend on what happens along the whole electron trajectory. If the demagnetization region is small the overall potential drop, affecting the demagnetized electrons, may be also too small to produce substantial energization. It is difficult (if possible at all) to study the global behavior of electron trajectories analytically, especially taking into account sensitivity to initial conditions. Nor it is possible to study the demagnetization in arbitrary geometry. We shall, therefore, perform a numerical analysis of electron trajectories in a model shock profile, bearing in mind that qualitative results should be applicable to any thin slowly varying structure. We shall put special emphasis on the changes in the electron distribution, depending of the shock width. To this end we specify the fields within the shock profile as in Gedalin and Balikhin (1998):

$$B_z = B_u \sin\theta \left[\frac{R+1}{2} + \frac{R-1}{2}\tanh\left(\frac{1.5x}{D}\right)\right], \quad (40)$$

$$B_y = \frac{c\cos\theta}{M\omega_{pi}}\frac{dB_z}{dx}. \quad (41)$$

These expressions describe only the shock ramp, where the demagnetization is most plausible. The other parts of the shock structure (foot, overshoot, and large amplitude downstream oscillations) are unlikely to be sufficiently narrow to allow electron demagnetization. While subsequent (or preceding in the foot) adiabatic motion of electrons in these regions would affect the shape of the electron distribution function, it would not change the conclusions about the demagnetized electron features, since these are determined only by their motion in the ramp. Being interested in the transition from completely magnetized electron motion to substantial demagnetization, we have to analyze only that part of the shock profile where such a transition can occur.

The approximation (41) has been shown to be rather imprecise for high Mach number shocks (Gedalin, 1996; Gosling et al., 1988; Jones and Ellison, 1987, 1991; Newbury et al., 1997a; Thomsen et al., 1987b), overestimating $B_y$ inside the ramp. However, we shall use it here, in the absence of a better model description, since no direct comparison with observations is planned. Higher $B_y$ results in the more fast increase of the total magnetic field inside the ramp, thus somewhat reducing the region where demagnetization can occur. Within the stationary one-dimensional shock model $B_y$, integrated over the ramp width, determines the normal incidence frame cross-shock potential, provided the de Hoffman-Teller potential is fixed by other parameters. Thus $\varphi^{(N)}$ does not depend on the details of the $B_y$ behavior in the ramp. To maintain the same normal incidence frame potential $B_y$ should increase with the ramp narrowing. There is some controversy in this issue since the observed $B_y$ are always substantially less than $B_z$. On the other hand, too low $\varphi^{(N)}$ would be inconsistent with the ion deceleration and reflection at the ramp (Wilkinson and Schwartz, 1990). It can be seen that the overestimated $B_y$ results in more significant increase of local $|\mathbf{B}|$ than $|\partial E_x \partial x|$, thus somewhat suppressing demagnetization. The tanh approximation used in (40) slightly overestimates $dB/dx$ in the middle of the ramp, whose width is approximately $2.5D$, but substantially underestimates $dB/dx$ and even more $d^2B/dx^2$ near the edges of the ramp. Real magnetic field profiles do not tend to zero so smoothly. We shall see that demagnetization occurs near the upstream edge of the ramp, so that the chosen profile is unfavorable for demagnetization, allowing it only for extremely narrow profiles.

As far as a stationary and one-dimensional model shock is considered, it is convenient to perform the numerical analysis in the de Hoffman-Teller frame. We shall specify the HT electric field as suggested by (9), assuming polytropic law $p \propto n^2$ for electrons, and $n/B = \mathrm{const}$, which gives

$$eE_x = -\frac{\beta_e B_u}{4\pi n_u}\frac{dB}{dx}. \quad (42)$$

$$e\phi = \frac{\beta_e B_u^2}{4\pi}\left(\frac{B}{B_u} - 1\right), \quad (43)$$

It is easy to see that approximately the demagnetization parameter $\alpha \propto (d^2B/dx^2)/B^2$. Our usage of the tanh profile for $B_z$ underestimates $d^2B/dx^2$ and overestimates $B_y$, which contributes into $B^2$, thus substantially underestimating $\alpha$ in this geometry. Therefore, the parameters used hereafter should not be compared directly to the observational shock parameters. The chosen model, however, is especially convenient for the present study, since the electron demagnetization is controlled by a single parameter, namely ramp

scale $D$, which is approximately 0.4 of the ramp width. Throughout the paper we use the following parameters: $M = 7.5$, $\theta = 76°$, and $R = 4$. We traced trajectories of initially Maxwellian distributed electrons ($\beta_e = 0.5$) for the following several values of the ramp scale $D = 5(c/\omega_{pe})$, $3(c/\omega_{pe})$, and $(c/\omega_{pe})$, the narrowest ramp width corresponding to $\approx 2.5(c/\omega_{pe})$.

The objective of the analysis is to numerically establish the relation between initial electron parallel and perpendicular velocities $v_{0,\parallel} = \mathbf{v}_0 \cdot \mathbf{B}_u/|\mathbf{B}_u|$, $v_{0,\perp} = (\mathbf{v}_0^2 - v_{0,\parallel}^2)^{1/2}$ and the corresponding downstream velocities $v_{d,\parallel} = \mathbf{v}_d \cdot \mathbf{B}_d/|\mathbf{B}_d|$, $v_{d,\perp} = (\mathbf{v}_d^2 - v_{d,\parallel}^2)^{1/2}$, where $\mathbf{v}_0$ is given in the far upstream region, and $\mathbf{v}_d$ is obtained in the far downstream region, where the fields can be considered homogeneous. We are not interested in retaining any information about the electron gyrophase, since the electron gyroradius is typically small compared to the length over which the distribution is effectively averaged during observations. Such information would be necessary for the consideration of the electron pressure tensor within the ramp, which is beyond the scope of the present paper.

In a wide ramp electrons are expected to behave adiabatically, that is,

$$v_{d,\perp}^2 = v_{0,\perp}^2(B_d/B_u), \tag{44}$$

$$v_{d,\parallel}^2 + v_{d,\perp}^2 = v_{0,\parallel}^2 + v_{0,\perp}^2 + \frac{2e\phi}{m_e}. \tag{45}$$

The last relation is more conveniently written as

$$v_{d,\parallel}^2 + v_{d,\perp}^2 = v_{0,\parallel}^2 + v_{0,\perp}^2 + 4v_{Te}^2[(B_d/B_u) - 1], \tag{46}$$

where we used (43) and $v_{Te}^2 = T_e/m_e = \beta_e B_u^2/8\pi n_u m_e$. One particular implication of (44) and (46) is that all electrons with the initial velocities, satisfying the relation

$$v_{0,\parallel}^2 < (v_{0,\perp}^2 - 4v_{Te}^2)(B_d/B_u - 1), \tag{47}$$

are reflected at the ramp.

In the numerical analysis the whole initial phase space of electrons is divided into four parts, according to the sign of their initial $v_{0,\parallel}$ and final $v_{f,\parallel}$ parallel velocities: (a) transmitted electrons, for which $v_{0,\parallel} > 0$ and $v_{f,\parallel} > 0$, (b) reflected electrons, for which $v_{0,\parallel} > 0$ and $v_{f,\parallel} < 0$, (c) another group of reflected electrons, for which $v_{0,\parallel} < 0$ and $v_{f,\parallel} > 0$ (these particles actually mirror the previous group and are not considered in the analysis), and (d) backstreaming electrons, for which $v_{0,\parallel} < 0$ and $v_{f,\parallel} < 0$, and which have to come from the downstream region to match the upstream electrons heading into upstream. Since we were interested only in the phase space transformation no weighting of downstream electrons according to their staying time has been done, so that the following figures show mapping of initial velocities into final velocities and *do not* show downstream electron distribution.

Figure 1 shows the phase space for the initial electron distribution and corresponding downstream electron velocities (for transmitted electrons only). The initial distribution of

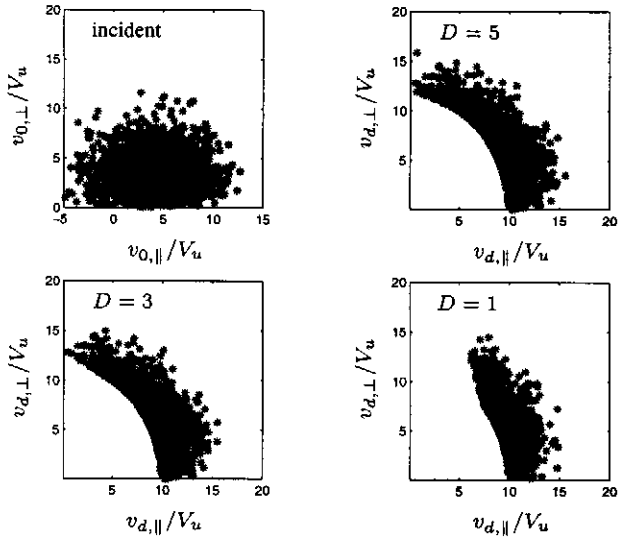


**Fig. 1.** Phase space $(v_\parallel, v_\perp)$ for initial electron distribution and corresponding downstream velocities of transmitted electrons for $D = 5$, 3, and 1 electron inertial lengths.

2000 Maxwellian distributed electrons is slightly supersonic in the de Hoffman-Teller frame, since $v_{Te}\cos\theta/V_u \approx 0.7$. The energies of the downstream electrons are limited from below by $e\phi$, that is, $v_{d,\parallel}^2 + v_{d,\perp}^2 > 4v_{Te}^2(B_d/B_u - 1)$. Downstream phase spaces for $D = 5$ and $D = 3$ (hereafter we measure $D$ in electron inertial lengths) are almost identical and match our expectations of what should be seen in the adiabatic case. In the case $D = 1$ the phase space portrait is substantially different. Low $v_\parallel$ electrons are absent, meaning stronger electron reflection in the demagnetized regime. We will consider the reflected electrons in more detail below. The electron energies clearly obey the energy conservation: $v_\parallel^2 + v_\perp^2 \geq 2e\phi/m_e$. Absence of transmitted electrons with low $v_\parallel$ means that some electrons acquire too high perpendicular energy during their demagnetization and are subsequently reflected by the increasing magnetic field, when they become magnetized again (Gedalin et al. , 1995b). It should be emphasized that this electron reflection depends strongly on the HT cross-shock potential. If the effective polytropic index $\gamma > 2$, as occurs in shocks with strong electron heating (Schwartz et al., 1988; Thomsen et al., 1987a), the cross-shock potential is higher, than predicted by (43), and reflection is suppressed.

Figure 2 shows the dependence of the downstream perpendicular velocity $v_{d,\perp}$ of transmitted electrons on their initial perpendicular velocity for the adiabatic case $D = 5$ and in the case of strong demagnetization $D = 1$. In the adiabatic case the dependence clearly follows the magnetic compression prescribed relation $v_{d,\perp} = \sqrt{B_d/B_u}\, v_{0,\perp}$. In the nonadiabatic case there is a large spread in downstream velocities, even for close initial perpendicular velocities. This spread is roughly independent of the initial perpendicular velocity and approximately corresponds to $2e\phi/m_e$. It is better seen in Figure 3, where the same mapping is shown for three cases, $D = 5$, $D = 3$, and $D = 1$, and low $v_{0,\perp} < 1$ elec-

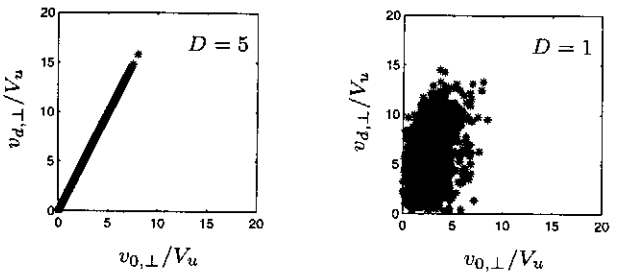


**Fig. 2.** Dependence of downstream perpendicular velocity $v_{d,\perp}$ on the initial perpendicular velocity $v_{0,\perp}$ of transmitted electrons for $D = 5$ and $D = 1$.

trons only, to exclude the magnetic compression effect. The difference between the adiabatic (and almost adiabatic) and strongly nonadiabatic cases is striking. In the adiabatic case there is a one-to-one correspondence $v_{0,\perp} \rightarrow v_{d,\perp}$, which is determined by the magnetic compression. In the nonadiabatic case this one-to-one correspondence no longer exists and is substituted by a visually chaotic scattering. This is in complete agreement with the previously shown strong dependence of the perpendicular energization on the initial gyrophase (Gedalin et al. , 1995b). Since we do not keep the gyrophase information this quasi-random energization would probably lead to the coarse-grained entropy production.

Of particular interest is the efficiency of the perpendicular energization, which can be expressed in terms of the ratio $v_{d,\perp}/\sqrt{B_d/B_u}v_{0,\perp}$. This ratio for the three cases as a function of the initial perpendicular velocity is shown in Figure 4. In the adiabatic case this ratio is constant and equals $\sqrt{B_d/B_u}$. In the nonadiabatic case the efficiency is typically twice as great as the magnetic compression efficiency, and even reaches values by an order of magnitude larger. The maximum efficiency for given $v_{0,\perp}$ is large for small initial perpendicular velocities and rapidly drops, approximately as $1/v_{0,\perp}$, when the initial perpendicular velocity increases. This result is in agreement with the conclusion that the maximum nonadiabatic perpendicular energization is determined by the cross-shock potential, $v^2_{d,\perp,\max} \approx 2e\phi/m_e \approx$ const, so that $v_{d,\perp}/\sqrt{B_d/B_u}v_{0,\perp} \sim \sqrt{2e\phi/m_e}/v_{0,\perp}$. It was shown earlier numerically (Balikhin and Gedalin, 1994) that perpendicular electron heating behaves in the similar way, which is also in agreement with observations (Schwartz et al., 1988).

To summarize, transmitted electrons, in the case of strong demagnetization, are energized in the perpendicular direction much more efficiently than in the adiabatic case. This energization only weakly depends on the initial perpendicular velocity of the electron, but is rather sensitive to its initial gyrophase. Since the amount of the total energy increase for any given electron is exactly the cross-shock potential energy, and is therefore constant, the adiabatic energization results in the regular redistribution of this energy among the parallel and perpendicular degrees of freedom, while the nonadiabatic mechanism introduces some randomness in this redistribution.

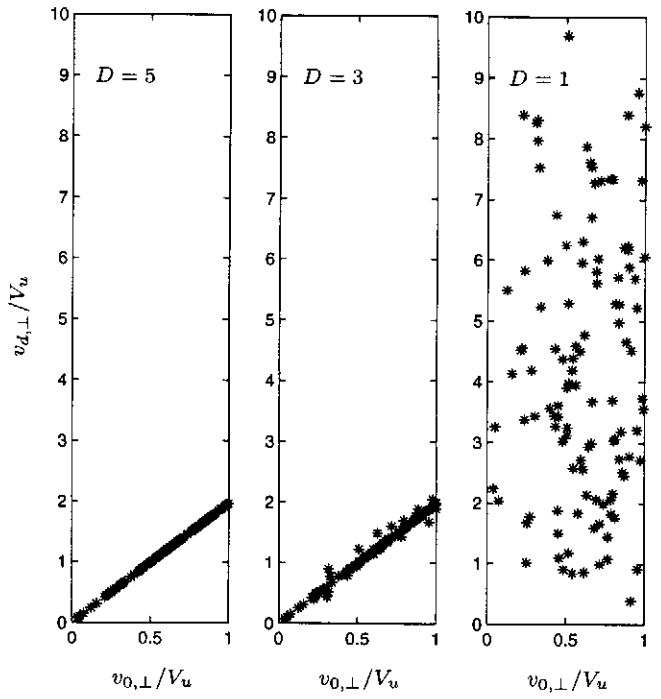


**Fig. 3.** Dependence of downstream perpendicular velocity $v_{d,\perp}$ on the initial perpendicular velocity $v_{0,\perp}$ of transmitted electrons with low initial perpendicular velocities, for $D = 5$, $D = 3$, and $D = 1$.

As was said above, electron reflection depends significantly on both ramp width and cross-shock potential. Figure 5 provides closer look at the initial phase space of those electrons which are reflected in the adiabatic case $D = 5$ and nonadiabatic case $D = 1$. It is clearly seen that the number of reflected electrons is larger in the nonadiabatic case, at the expense of electrons, which have low initial $v_{0,\perp}$. That means, that the enhanced reflection is due to the strong perpendicular energization of these electrons in the upstream part of the ramp (where demagnetization occurs) with subsequent magnetic reflection deeper in the ramp. During this reflection the perpendicular energy is transferred into the parallel degree of freedom. However, since the initial energization differs from the magnetic compression produced energization, these reflected electrons would have finally perpendicular energies different from the initial values. This expectation is confirmed by direct numerical analysis, as shown in Figure 6, where the final perpendicular velocities of reflected electrons $v_{r,\perp}$ are plotted against their initial perpendicular velocities $v_{0,\perp}$. In both case velocities are measured far upstream before and after the interaction with the ramp fields. It is clearly seen that the reflected ion beam has some spread in $v_\perp$. The result of this combination of demagnetization with magnetic mirroring is shown in Figure 7, where the electron initial velocities (absolute values) are shown by circles, and their final velocities are shown by crosses. The initial and final velocities completely coincide in the case $D = 5$, where only magnetic mirroring works. In the case $D = 1$ the electrons have typically higher perpendicular velocities and lower parallel

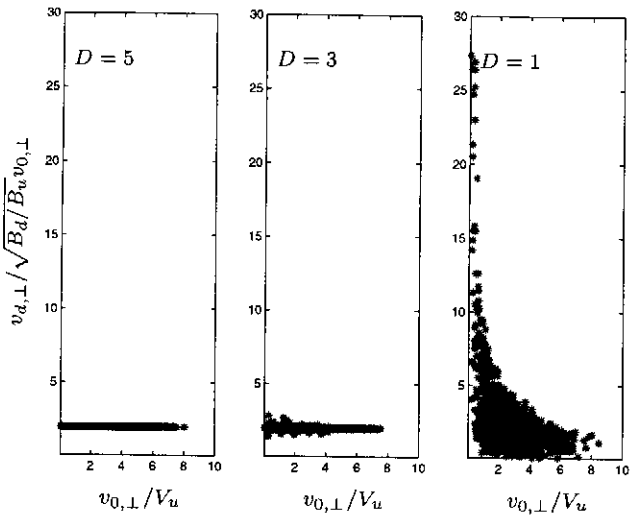


**Fig. 4.** Perpendicular energization efficiency in the three cases.

velocities after the reflection than before.

Finally, Figure 8 shows the velocities of the electrons which cross the ramp from downstream to upstream to match the corresponding phase space in the incident Maxwellian distribution. It is clearly seen that there are less those electrons in the nonadiabatic case, which is obviously related to the stronger reflection.

## 5 Discussion and conclusions

To summarize, we have shown that it is likely that in thin shocks electrons are demagnetized at least in the part of the shock ramp. We have shown that the electric field component in the direction of the largest gradient is determined primarily by the requirement of the electron balance. This conclusion is correct even if the structure is not exactly one-dimensional and stationary, and when then the N-HT relations are not useful, provided that the typical time scale of the field variations is much larger than the electron gyroperiod, and that the structure is locally planar. We have analyzed the demagnetization condition in general case, without assuming stationarity and one-dimensionality, and have shown that strong demagnetization occurs when rather small deviations from quasineutrality occur. We have argued that the features of electron demagnetization (and dynamics in general) within the shock ramp should be similar to what electrons experience in short scale large amplitude structures, even if they are not stationary and one dimensional. Thus, studying electron motion in the shock front provides some insight into features of electron interaction with inhomogeneous fields in other systems.

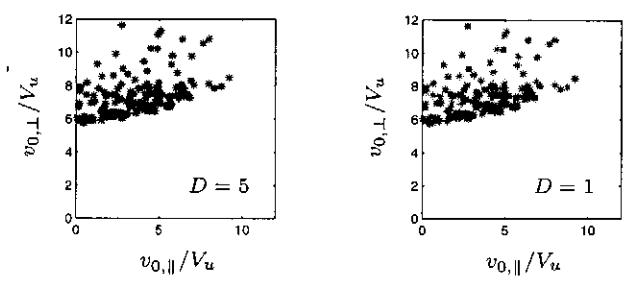


**Fig. 5.** Initial velocities of electrons that are reflected in the case $D = 5$ and $D = 1$.

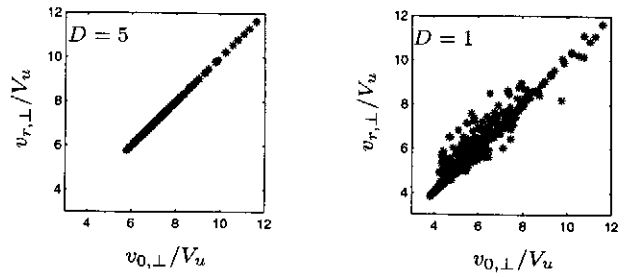


**Fig. 6.** Final perpendicular velocities of reflected electrons vs their initial perpendicular velocities.

Using analysis of electron trajectories in a model shock profile, we have shown that in the case of a thin shock ramp all electrons demagnetization does not depend much on the initial ion parallel or perpendicular velocities, which manifests itself in the almost equal spread in the acquired perpendicular energies for all initial perpendicular velocities of the incident electrons. The perpendicular energy gain depends strongly on the initial electron gyrophase, which is not measured in real observations. The relative perpendicular energy gain decreases with the increase of the initial perpendicular velocity, what is responsible for the drop of the nonadiabatic energization efficiency for these electrons. We have shown that the electron reflection also becomes nonadiabatic in thin shocks, and that the number and distribution of reflected electrons is sensitive to the shock width and cross-shock potential.

Our usage of the oversimplified model of the shock front (monotonic ramp only) is justified because of the observation that the electron motion should be almost completely adiabatic in other parts (foot, overshoot, and large amplitude downstream oscillations) of the shock structure, which means that the demagnetization properties are determined only by the field distribution in the ramp. The other parts of the shock structure will participate adiabatically in the formation of the eventual electron distribution. This distri-

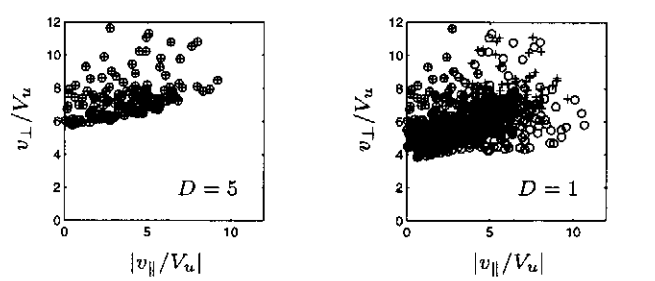


**Fig. 7.** Initial (circles) and final (crosses) velocities of reflected electrons.

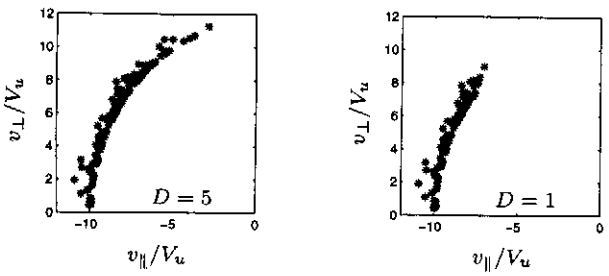


**Fig. 8.** Downstream velocities of backstreaming electrons.

bution would be also affected by deviations from one-dimensionality within the shock front and non-stationarity of the field, as well as by large amplitude waves and turbulence. Nevertheless, those features, which are due to electron demagnetization, should be similar to what has been found in the present analysis. Recent study by Newbury et al. (1997b) shows that the shock ramp itself can contain quasi-stationary or slowly varying fine scale substructure with the typical scale of 0.1-0.2 $(c/\omega_{pi})$. In this case the results obtained here would be applicable to the description of the electron behavior in this substructure. In any case, comparison with observations would require better knowledge of the field distribution in real shocks and better understanding of the shock structure formation and stability. One of the important unresolved issues is turbulent smoothing of the collisionless electron distribution, which requires analysis of the stability of the magnetized and demagnetized electron distributions within the ramp.

*Acknowledgements.* The research was supported in part by Israel Science Foundation under grant No. 261/96-1.

## References

Balikhin, M., Krasnosel'skikh, V.V., Woolliscroft, L.J.C., and Gedalin, M., A study of the dispersion of the electron distribution in the presence of $E$ and $B$ gradients: application to electron heating at quasi-perpendicular shocks, *J. Geophys. Res.*, in press (1998).

Balikhin, M., Gedalin, M., and Petrukovich, A., New mechanism for electron heating in shocks, *Phys. Rev. Lett., 70*, 1259-1261, 1993.

Balikhin, M. and Gedalin, M., Kinematic mechanism for shock electron heating: comparison of theoretical results with experimental data, *Geophys. Res. Lett., 21*, 841-844, 1994.

Cole, K.D., Effects of crossed magnetic and (spatially dependent) electric fields on charged particle motion, *Planet. Space Sci., 24*, 515-518, 1976.

de Hoffman, F., and Teller, E., Magneto-hydrodynamic shocks, *Phys. Rev., 80*, 692-, 1950.

Feldman, W.C., Bame, S.J., Gary, S.P., Gosling, J.T., McComas, D., Thomsen, M.F., Paschmann, G., Sckopke, N., Hoppe, M.M., and Russell, C.T., Electron heating within the earth's bow shock, *Phys. Rev. Lett., 49*, 199-201, 1982.

Feldman, W.C., Electron velocity distributions near collisionless shocks, in *Collisionless Shocks in the Heliosphere: Reviews of Current Research, Geophys. Monogr. Ser.*, vol. 35, edited by R.G. Stone and B.T. Tsurutani, pp. 195–205, AGU, Washington, D. C., 1985.

Formisano, V., Measurement of the potential drop across the earth's collisionless bow shock, *Geophys. Res. Lett., 9*, 1033-1036, 1982.

Gedalin, M., Balikhin, M., and Krasnoselskikh, V., Electron heating in collisionless shocks, *Adv. Space Res., 15(8/9)*, 225–233, 1995a.

Gedalin, M., Gedalin, K., Balikhin, M., and Krasnoselskikh, V.V., Demagnetization of electrons in the electromagnetic field structure, typical for oblique collisionless shock front, *J. Geophys. Res., 100*, 9481–9488, 1995b.

Gedalin, M., Gedalin, K., Krasnoselskikh, V.V., Balikhin, M., and Woolliscroft, L.J.C., Demagnetization of electrons in inhomogeneous $\mathbf{E} \perp \mathbf{B}$: Implications for electron heating in shocks, *J. Geophys. Res., 100*, 19,911–19,918, 1995c.

Gedalin, M., Noncoplanar magnetic field in the collisionless shock front, *J. Geophys. Res., 101*, 11,153–11,156, 1996.

Gedalin, M., Gedalin K., Krasnoselskikh V.V., Balikhin M., and Woolliscroft L.J.C., Reply, *J. Geophys. Res., 101*, 2567-2569, 1996.

Gedalin, M., Newbury, J.A., and Russell, C.T., Shock profile analysis using wavelet transform, *J. Geophys. Res.*, in press (1998).

Gedalin, M. and Balikhin, M.A., Width dependent collisionless electron dynamics in the static field of the shock ramp, 1, Single particle behavior and implications for downstream distribution, (this issue).

Goodrich, C.C., and Scudder, J.D., The adiabatic energy change of plasma electrons and the frame dependence of the cross-shock potential at collisionless shock waves, *J. Geophys. Res., 89*, 6654-6662, 1984.

Gosling, J.T., Winske, D., and Thomsen, M.F., Noncoplanar magnetic fields at collisionless shocks: A test of a new approach, *J. Geophys. Res., 93*, 2735-2738, 1988.

Jones, F.C., and Ellison, D.C., Noncoplanar magnetic fields, shock potentials, and ion deflection, *J. Geophys. Res., 92*, 11,205–11,207, 1987.

Jones, F.C., and D.C. Ellison, The plasma physics of shock acceleration, *Space Sci. Rev., 58*, 259–346, 1991.

Krauss-Varban, D., F.G.E. Pantellini, and D. Burgess, Electron dynamics and whistler waves at quasi-perpendicular shocks, *Geophys. Res. Lett., 22*, 2091–2094, 1995.

Liewer, P.C., V.K. Decyk, J.M. Dawson, and B. Lembege, Numerical studies of electron dynamics in oblique quasi-perpendicular collisionless shock waves, *J. Geophys. Res., 96*, 9455–9465, 1991.

Newbury, J.A. and Russell, C.T., Observations of a very thin collisionless shock, *Geophys. Res. Lett., 23*, 781–784, 1996.

Newbury, J.A., Russell, C.T., and Gedalin, M., The determination of shock ramp width using the noncoplanar magnetic field component, *Geophys. Res. Lett., 24*, 1975–1978, 1997a.

Newbury, J.A., Russell, C.T., and Gedalin, M., Ramp scales of supercritical quasi-perpendicular bow shocks, *EOS Trans. AGU, 78*(46), Fall Meet. Suppl., F453, 1997b.

Quest, K.B., Simulations of high Mach number collisionless perpendicular shocks, *Phys. Rev. Lett., 54*, 1872–1875, 1985.

Rothwell, P.L., Silevitch, M.B., Block, L.P., and Falthammar, C.-G., Particle dynamics in a spatially varying electric field, *J. Geophys. Res., 100*, 14875–14885, 1995.

Savoini, P., and B. Lembege, Electron dynamics in two- and one-dimensional oblique supercritical collisionless magnetosonic shocks, *J. Geophys. Res., 99*, 6609–6635, 1994.

Schwartz, S.J., Thomsen, M.F., Bame, S.J., and Stansbury, J., Electron heating and the potential jump across fast mode shocks, *J. Geophys. Res., 93*, 12,923–12,931, 1988.

Scudder, J.D., A review of the physics of electron heating at collisionless shocks, *Adv. Space Res., 15(8/9)*, 181–223, 1995.

Scudder, J.D., Mangeney, A., Lacombe, C., Harvey, C.C., Aggson, T.L., Anderson, R.R., Gosling, J.T., Paschmann, G., and Russell, C.T., The resolved layer of a collisionless, high $\beta$, supercritical, quasi-perpendicular shock wave, 1, Rankine-Hugoniot geometry, currents, and stationarity, *J. Geophys. Res., 91*, 11,019–11,052, 1986a.

Scudder, J.D., Mangeney, A., Lacombe, C., Harvey, C.C., and Aggson, T.L., The resolved layer of a collisionless, high $\beta$, supercritical, quasi-perpendicular shock wave, 2, Dissipative fluid electrodynamics, and stationarity, *J. Geophys. Res., 91*, 11,053–11,073, 1986b.

Scudder, J.D., Mangeney, A., Lacombe, C., Harvey, C.C., Wu, C.S., and Anderson, R.R., The resolved layer of a collisionless, high $\beta$, supercritical, quasi-perpendicular shock wave, 3, Vlasov electrodynamics, *J. Geophys. Res., 91*, 11,075–11,097, 1986c.

Tabor, M., Chaos and integrability in nonlinear dynamics : an introduction,

Wiley, New York, 1989.

Thomsen, M.F., Mellott, M.M., Stansbury, J.A., Bame, S.J., Gosling, J.T., and Russell, C.T., Strong electron heating at the Earth's bow shock, *J. Geophys. Res., 92,* 10,119–10,124, 1987a.

Thomsen, M.F., Gosling, J.T., Bame, S.J., Quest, K.B., Winske, D., Livesey, W.A., and Russell, C.T., On the noncoplanarity of the magnetic field within a fast collisionless shock, *J. Geophys. Res., 92,* 2305–2314, 1987b.

Wilkinson, W.P., and S.J. Schwartz, Parametric dependence of the density of specularly reflected ions at quasiperpendicular collisionless shocks, *Planet. Space Sci., 38,* 419–435, 1990.

Wygant, J.R., Bensadoun, M., and Mozer, F.C., Electric field measurements at subcritical, oblique bow shock crossings, *J. Geophys. Res., 92,* 11,109–11,121, 1987.